Journal of Balkan Science and Technology
journal homepage: www.jbst.nku.edu.tr/

Analytical Solution of Bending, Buckling, and Vibration of Functionally Graded Nanobeams based on Nonlocal Elasticity

Bahar UYMAZ[1*]

[1]*Tekirdağ Namık Kemal University, Faculty of Engineering, Department of Mechanical Engineering, 59860, Corlu-Tekirdağ, Türkiye*

Research Article

Keywords:
Nonlocal elasticity
Functionally graded nanobeam
Bending
Buckling
Free vibration

Received:25.03.2023
Accepted:29.04.2023
Published:30.04.2023

DOI: 10.55848/jbst.2023.29

ABSTRACT

Navier solution presented for bending, buckling, and free vibration of simply supported functionally graded nanobeams based on generalized shear deformation theory. The results are obtained for parabolic shear deformation theory corresponding to Reddy beam theory using nonlocal differential constitutive equations which were formulated by Eringen [1,2,3]. The material properties of the functionally graded nanobeam vary through the thickness direction according to a simple power law. Effects of the nonlocal parameter, different material composition and length-to-thickness ratio on the maximum deflection, critical buckling load, and natural frequencies of the nanobeam are investigated. The results show that the scale effects, material composition, and dimensional changes are affected by considered parameters. Nonlocal elasticity theory predicts softening material behavior compared to classical elasticity theory because it takes into account the effects of long-range interactions between material particles. As a result of this, the maximum deflections, critical buckling loads, and natural frequencies obtained by the classical theory are higher than obtained by the nonlocal theory in all considered conditions.

1. Introduction

Classical elasticity assumes that the stress at a point depends only on the local deformation of the material. However, nonlocal elasticity accepts that the stress at a point also depends on the deformation of neighboring points, which are weighted according to a nonlocal kernel function unlike classical elasticity [1,2,3]. The non-local approach is particularly useful for modeling materials with non-local effects, such as nanomaterials and biological tissues, where the interactions between particles are not limited to the immediate vicinity of a point, but can also be an effective approach for wave propagation, fracture behavior, and stability of structures. Nonlocal elasticity has been applied in a variety of fields, including materials mechanics, structural engineering, and biomechanics, although its formulation is more complex than classical elasticity and requires numerical techniques to solve governing equations.

There are many presented analytical solutions on the mechanical behavior of nanobeams such as bending, buckling, and vibration based on Euler-Bernoulli beam theory and Timoshenko beam theory, which in the framework of nonlocal constitutive relation proposed by Eringen. Reddy [4] presented an analytical solution of bending, buckling, and vibration of nanobeams using various beam theories including the Euler-Bernoulli, Timoshenko, Reddy, and Levinson beam theories based on the nonlocal elasticity. Thai [5] proposed a nonlocal shear deformation theory for bending, buckling, and vibration of nanobeams using the nonlocal differential constitutive relations of Eringen. According to the theory, shear strains and consequently shear stresses vary quadratically through the thickness. The Euler-Bernoulli, Timoshenko, Reddy, Levinson, and Aydogdu beam theories are used as a special case by Aydogdu [6] on bending, buckling, and vibration of nanobeams. Ghannadpour et al. [7] investigated bending, buckling, and vibration based on nonlocal Euler-Bernoulli beam theory using Ritz method. Wang et al. [8] concerned with the bending problem of micro- and nanobeams based on the Eringen nonlocal elasticity theory and Timoshenko beam theory. Lu et al. [9] used nonlocal Euler-Bernoulli beam theory for vibration analysis of nanobeams.

Li et al. [10] considered the free vibration of nonlocal Euler and Timoshenko beams. It was provided a novel explanation for the stiffening phenomenon of nonlocal cantilever beams, clarified the effects of local and nonlocal boundary conditions on the free vibration, and revealed the effects of different constitutive relations for nonlocal Timoshenko beams. Wang et al. [11] concerned with the free vibration problem for micro/nanobeams modeled after Eringen's nonlocal elasticity theory and Timoshenko beam theory.

Thai and Vo [12] used a sinusoidal shear deformation beam theory which is capable of capturing both small-scale effect and transverse shear deformation effects of nanobeams, and does not require shear correction factors for the bending,

[*] *Tekirdağ Namık Kemal University, Faculty of Engineering, Department of Mechanical Engineering, 59860, Corlu-Tekirdağ, Türkiye*
E-mail address: buymaz@nku.edu.tr

buckling, and vibration of nanobeams. Eltaher et al. [13] used an efficient finite element model for dynamic characteristics analysis of a nonlocal Euler–Bernoulli nanobeam. Roque et al. [14] used the nonlocal elasticity theory of Eringen to study bending, buckling, and free vibration of Timoshenko nanobeams. A meshless method was presented to obtain numerical solutions.

Functionally graded materials (FGMs) are a class of engineered materials that are designed to have spatial variations in their composition and/or microstructure to achieve specific mechanical, thermal, electrical, or other properties. Unlike traditional materials, which have uniform properties throughout their volume, FGMs exhibit a gradual or abrupt transition in their properties along one or more directions [15]. The concept of FGM was first developed by Japanese researchers in the 1980s as materials capable of withstanding the extreme temperature changes were encountered in aerospace applications but has since found a wide range of applications in fields such as aerospace, energy, biomedical engineering, and materials science. While FGMs can be designed to exhibit a variety of property gradients, such as variations in composition, porosity, grain size, and fiber orientation, the composition gradient is the most common type of gradient. The composition gradient involves a gradual change in the type or concentration of one or more constituents of the material as in the example of a metal-ceramic FGM which has a gradient in the concentration of ceramic particles increasing from one end of the material to the other.

Although the design and fabrication of FGMs can be challenging and require advanced materials processing techniques, they have a wide range of potential application areas due to their several advantages over traditional homogeneous materials, such as improved fracture resistance, reduced stress concentration, and enhanced thermal shock resistance. FGM structures which can be designed and optimized for specific applications by tailoring their composition and properties have a wide range of applications such as aircraft and spacecraft components, missile components, armor plating, dental implants, prosthetics, bone grafts, fuel cells and batteries, heat sinks and heat exchangers, bridges, buildings, and other civil engineering structures.

There are many studies in the literature dealing with bending, buckling, and free vibration of functionally graded beams [16-29]. With this, bending, buckling, and free vibration are important mechanical behaviors that need to be analyzed in order to design and optimize functionally graded nanobeam structures for various nano applications. Eltaher et al. [30] presented a free vibration analysis of functionally graded size-dependent nanobeams using a finite element method based on nonlocal Euler-Bernoulli beam theory. Simsek and Yurtcu [31] investigated static bending under uniformly distributed load and buckling analysis of functionally graded nanobeams based on nonlocal Timoshenko beam theory that first-order shear deformation theory. Buckling results and vibration results of functionally graded nanobeams based on Reddy theory were presented by Rahmani and Jandaghian [32] and Ebrahimi and Barati [33], respectively. Explicit analytical equations for the vibration of a bidirectional functionally graded nonlocal nanobeam are presented by Nazmul et al. [34].

However, it is seen that the effect of Poisson ratio was not taken into account in these studies on functionally graded nanobeams. However, the Poisson ratio is a measure of the deformation of a material in response to an applied force. It is defined as the ratio of the lateral strain to the longitudinal strain in a material when it is stretched or compressed. In other words, it is a measure of how much a material will shrink or expand perpendicular to the direction of an applied force. The value of Poisson's ratio is an important factor in determining the mechanical behavior of materials under stress, as it affects their elastic modulus, shear modulus, and other mechanical properties. It becomes even more important to consider the effect of Poisson ratio in functionally graded materials where mechanical properties such as elastic modulus, density, and Poisson ratio vary across thickness. The static bending, the buckling, and the free vibration of the functionally graded nanobeam with the effect of Poisson's ratio taken into account is the subject of this paper. In this study, the generalized shear deformation theory with the shape function corresponding to the Reddy theory is used based on the nonlocal elasticity theory. The material properties of the functionally graded nanobeam assumed to vary in the thickness direction. The Navier-type solution is used for simply-supported boundary conditions, and exact formulas are proposed for the maximum deflections, the critical buckling load, and the natural frequencies. The effects of the nonlocal parameter ($(e_0a)^2$), the material composition (p index), and the length-to-thickness ratio (L/h) on the static, the stability and free vibration responses of the functionally graded nanobeam are discussed.

2. Theoretical formulations

2.1 Nonlocal elasticity theory

According to nonlocal elasticity theory, different from the classical elasticity theory, the stress field at a point x in an elastic continuum not only depends on the strain field at the same point but also on strains at all other points of the body. As a result of this, in classical elasticity theory, the behavior of a material is described purely in terms of its local properties, such as its stiffness and strength. However, in nonlocal elasticity theory, the behavior of a material is also affected by the material's microstructure, such as the size and shape of its particles. Nonlocal elasticity theory introduces a length scale parameter known as the nonlocal parameter, which is related to the material's microstructure. The presence of this length scale parameter causes the stress and strain in a material to be more distributed over a larger area, which leads to a reduction in the overall stiffness of the material. This effect is particularly pronounced in materials with a high surface area-to-volume ratio, such as nanomaterials. Therefore, nonlocal elasticity theory predicts that the material will be less stiff and less resistant to deformation than classical elasticity theory. In other

words, the material will exhibit a softer response to external loads.

The nonlocal stress tensor σ at point **x** is defined as follows:

$$\sigma(x) = \int_v \alpha(|x' - x|, \tau) t(x') dv(x') \quad (1)$$

$$t(x) = C(x) : \varepsilon(x) \quad (2)$$

where t(x′) is the classical, macroscopic stress tensor at point x, α(|x′-x|,τ) is the Kernel function and τ is the material constant which depends on a constant appropriate to each material (e_0), internal characteristic (a) such as lattice parameter, granular distance and external characteristic length (l) such as crack length, wavelength. With the reduced and simplified differential form of Eq. (1) and using Eq. (2) the relationship between classical, macroscopic stress tensor t and nonlocal stress tensor σ is given by Laplacian operator ∇ as follows:

$$(1 - \tau^2 l^2 \nabla^2)\sigma = C(x) : \varepsilon(x) \qquad \tau = \frac{e_0 a}{l} \quad (3)$$

It is seen that when the internal characteristic length a is zero, nonlocal elasticity corresponds to classical elasticity.

2.2 Governing equations of functionally graded nanobeams

The considered functionally graded nanobeam is a straight prismatic beam with length L along the x-axis and thickness h along the z-axis. The governing equations in terms of reduced stiffness coefficients, including Poisson's ratio effects, are as follows:

$$(1 - (e_0 a)^2 \frac{d^2}{dx^2})\sigma_x = Q_{11}\varepsilon_x$$

$$(1 - (e_0 a)^2 \frac{d^2}{dx^2})\tau_{xz} = Q_{55}\gamma_{xz} \quad (4)$$

Where Qij are the reduced stiffness coefficients defined according to FGMs as follows:

$$Q_{11} = \frac{E(z)}{1 - \nu(z)^2}, \qquad Q_{55} = \frac{E(z)}{2(1 + \nu(z))} \quad (5)$$

The displacement model of the beam defined according to the generalized shear deformation theory, as the axial displacement defined at any point, w_1 and the vertical displacement w_3 are as follows:

$$w_1 = u(x;t) - z\frac{\partial w}{\partial x} + f(z)u_1(x;t)$$

$$w_2 = 0$$

$$w_3 = w(x;t) \quad (6)$$

where u and w are the displacement components of a point on the mid-plane of the beam along the x- and z- axis, respectively. And f(z) is the transverse shear shape function which determines the distribution of the transverse shear strains and stresses throughout the beam thickness. Frequently used shape functions and derivatives along with their corresponding theories are given in Table 1 and illustrated in Fig.1.

Table 1. The mostly used transverse shape functions and derivatives along with their corresponding theories.

Shape function	Derivative of shape function	Corresponding theory
$\mathbf{f(z) = 0}$	$\frac{df}{dz} = 0$	Euler-Berrnoulli beam theory (EBT)
$\mathbf{f(z) = z}$	$\frac{df}{dz} = 1$	Timoshenko beam theory (TBT)
$\mathbf{f(z) = z\left(1 - \frac{4z^2}{3h^2}\right)}$	$\frac{df}{dz} = 1 - \frac{4z^2}{h^2}$	Reddy beam theory (RBT)
$\mathbf{f(z) = z3^{\frac{-2(z/h)^2}{\ln 3}}}$	$\frac{df}{dz} = 3^{\frac{-2(z/h)^2}{\ln 3}}\left(1 - \frac{4z^2}{h^2}\right)$	Aydogdu beam theory (ABT)

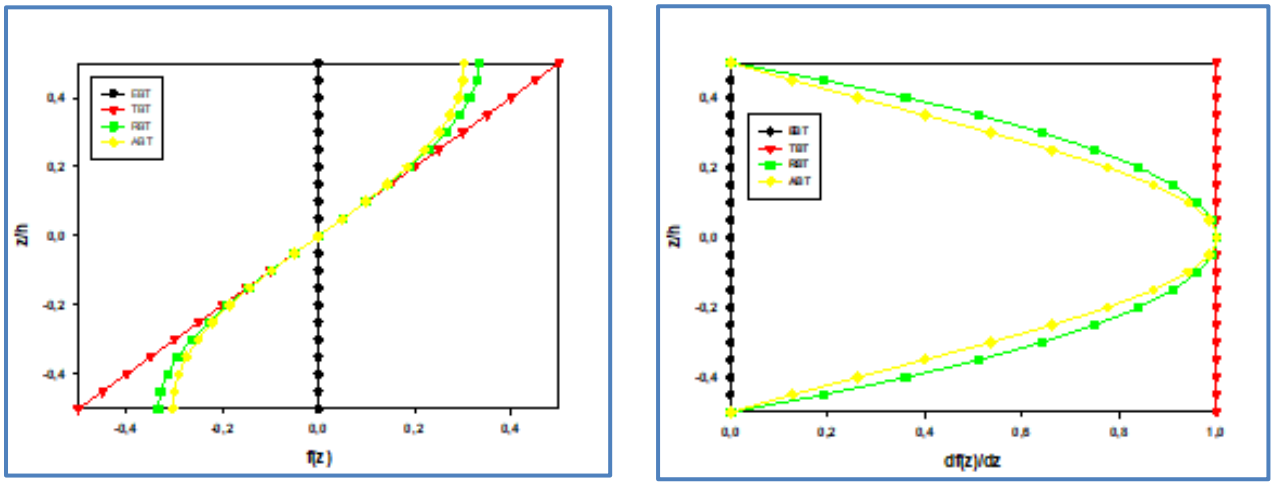

Fig 1. Variation of the frequently used (a) transverse shape functions and (b) derivatives along with their corresponding theories throughout the thickness coordinate.

The strain components in terms of the displacement components are as follows:

$$\varepsilon_x = \frac{\partial u}{\partial x} - z\frac{\partial^2 w}{\partial x^2} + f(z)\frac{\partial u_1}{\partial x}$$

$$\gamma_{xz} = \frac{df}{dz}u_1 \tag{7}$$

The internal force and moment resultants are as follows:

$$(N_x^c, M_x^c) = \int_{-h/2}^{h/2} \sigma_x(1, z)dz$$

$$M_x^{sd} = \int_{-h/2}^{h/2} \sigma_x f(z)dz$$

$$Q_x^{sd} = \int_{-h/2}^{h/2} \tau_{xz}(\frac{df}{dz})dz \tag{8}$$

The constitutive relations are as follows:

$$\begin{Bmatrix} N_x^c \\ M_x^c \\ M_x^{sd} \end{Bmatrix} = \begin{bmatrix} A_{11} & B_{11} & E_{11} \\ B_{11} & D_{11} & F_{11} \\ E_{11} & F_{11} & H_{11} \end{bmatrix} \begin{Bmatrix} u_{,x} \\ -w_{,xx} \\ u_{1,x} \end{Bmatrix}$$

$$\{Q_x^{sd}\} = [A_{55}]\{u_1\} \tag{9}$$

The extensional, coupling, bending, and transverse shear rigidities are as follows:

$$(A_{11}, B_{11}, D_{11}) = \int_{-h/2}^{h/2} Q_{11}(1, z, z^2)dz$$

$$(E_{11}, F_{11}, H_{11}) = \int_{-h/2}^{h/2} Q_{11} f(z)(1, z, f(z))dz$$

$$A_{55} = \int_{-h/2}^{h/2} Q_{55}(\frac{df}{dz})^2 dz \tag{10}$$

The governing equations of nanobeam obtained using principle of virtual work are as follows:

$$\frac{\partial N_x^c}{\partial x} = (1 - (e_0 a)^2 \frac{\partial^2}{\partial x^2})\left(\rho_0 \frac{\partial^2 u}{\partial t^2} - \rho_1 \frac{\partial^3 w}{\partial x \partial t^2} + \rho_{01}\frac{\partial^2 u_1}{\partial t^2}\right)$$

$$\frac{\partial^2 M_x^c}{\partial x^2} = (1 - (e_0 a)^2 \frac{\partial^2}{\partial x^2})\left(\rho_0 \frac{\partial^2 w}{\partial t^2} + \rho_1 \frac{\partial^3 u}{\partial x \partial t^2} - \rho_2 \frac{\partial^4 w}{\partial x^2 \partial t^2} + \rho_{11}\frac{\partial^3 u_1}{\partial x \partial t^2} - N_x^e \frac{\partial^2 w}{\partial x^2} - q(x;t)\right)$$

$$\frac{\partial M_x^{sd}}{\partial x} - Q_x^{sd} = (1 - (e_0 a)^2 \frac{\partial^2}{\partial x^2})\left(\rho_{01} \frac{\partial^2 u}{\partial t^2} - \rho_{11} \frac{\partial^3 w}{\partial x \partial t^2} + \rho_{02}\frac{\partial^2 u_1}{\partial t^2}\right) \tag{11}$$

Where inertia terms are as follows:

$$\rho_i = \int_{-h/2}^{h/2} \rho(z) z^i dz \qquad (i=0,1,2)$$

$$\rho_{jm} = \int_{-h/2}^{h/2} \rho(z) z^j f_j^m dz \quad (j=0,1\ ;\ m=1,2) \tag{12}$$

Where ρ is the mass per unit volume.

2.3. Functionally graded materials

The considered structural element is a straight prismatic functionally graded nanobeam having length L along the x-axis and thickness h along the z-axis. Effective material properties elasticity modulus (E), Poisson ratio (υ) and mass density (ρ) are varying in the thickness direction according to a simple power law distribution defined as follows:

$$P_{eff} = V_U P_U + V_L P_L$$

$$V_U + V_L = 1$$

$$V_U = \left(\frac{z}{h} + \frac{1}{2}\right)^{p_z}$$

$$P_{eff} = \left(\frac{z}{h} + \frac{1}{2}\right)^{p_z} P_U + (1 - \left(\frac{z}{h} + \frac{1}{2}\right)^{p_z})P_L \tag{13}$$

where Peff corresponding to the effective material property, the subscript U and L corresponding to the material property of the upper and lower surface, respectively. In this study upper surface material ceramic rich and lower surface material metal rich are preferred. Variation of the volume fraction VU through the thickness direction of the functionally graded nanobeam is given in Fig.2 where VU is the volume fraction of the ceramic; and pz is the volume fraction exponent, 0≤pz≤∞. Different value of the volume fraction of VU corresponds to different distribution of material composition on functionally graded nanobeam: e.g. if that value is 0, material of the nanobeam is ceramic; if that value is 1, the variation of the volume fraction of the ceramic is linear from lower surface to upper surface. If the ceramic volume ratio is different from 0 and 1, variation of the material composition is nonlinear.

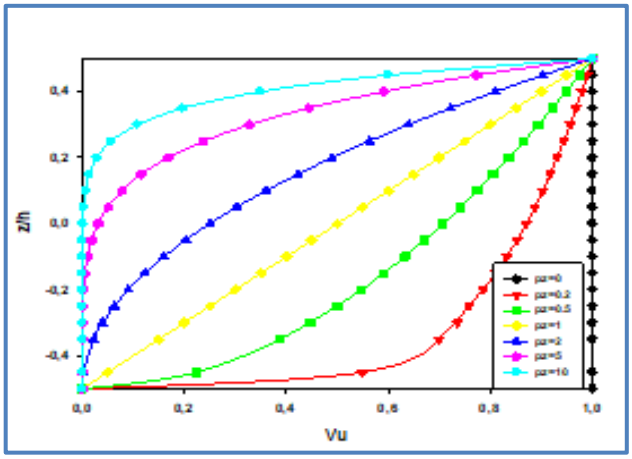

Fig.2. Variation of the volume fraction VU (ceramic component) through the thickness direction of the functionally graded nanobeam.

2.4 Analytical solution for bending, buckling, and free vibration of simply supported functionally graded nanobeam

In this study Navier method is applied for static bending, buckling, and free vibration problem of functionally graded nanobeam. The sets of boundary conditions of the beam at x=0, L are as follows:

either u or $N_x^c = \bar{N}_x$

either w or $M_{x,x}^c = \bar{Q}_x$

either w_x or $M_x^c = \bar{M}_x$

either u_1 or $M_x^a = \bar{M}_x^a$ (14)

where $\bar{N}_x$, $\bar{Q}_x$, $\bar{M}_x$, $\bar{M}_x^a$ are corresponding to prescribed force and moment resultants acting on the beam boundaries.

The simply supported boundary conditions of nanobeam are as follows:

$$N_x^c = w = M_x^c = M_x^a = 0 \quad (15)$$

The nanobeam equations given by Eq.(11) are organized as the external force (Nxe) term, and time dependent terms are zero on bending problem. Similarly the equations are organized as the time dependent terms and transverse load (q(x;t)) term are zero on buckling problem. Similarly the equations are organized as the external force (Nxe) term and transverse load (q(x;t)) term are zero on free vibration problem.

The kinematic components that provide the simply supported boundary condition in the bending and buckling analysis of the nanobeam examined are as follows:

$$u(x) = A_m \cos\frac{m\pi x}{L}$$

$$w(x) = C_m \sin\frac{m\pi x}{L}$$

$$Lu_1(x) = D_m \cos\frac{m\pi x}{L} \quad (16)$$

where u and w are the displacement components of a point in the midplane in the x and z directions; and u1 is the displacement components showing effects of vertical shear strains in the midplane. For bending analysis, the transverse load that provides the simply supported boundary condition is defined in the Fourier series form as follows:

$$q(x) = \sum_{m=1}^{M} Q_m \sin\frac{m\pi x}{L}$$

$$Q_m = \frac{2}{L}\int_0^L q(x)\sin\frac{m\pi x}{L}dx \quad (17)$$

Considered two types of loading that one of uniformly distributed load and one of point load condition in bending analysis are defined as follows:

Uniformly distributed load;

$$q(x) = q_0,\ Q_m = \frac{4q_0}{m\pi}(-1)^{m-1}, (m = 1,3,5,\dots),\quad Q_m = 0 \quad (m = 2,4,6,\dots) \quad (18)$$

Point load applied to point x0 from x=0 to L:

$$q(x) = q_0, \quad Q_m = \frac{2q_0}{L}\sin\frac{m\pi x_0}{L}, \quad (m = 1,2,3,\dots) \quad (19)$$

Firstly by substituting of the expansions Eq.(16) and Eq.(17) into Eq.(11) and then by applying non-dimensionalization procedure, max deflection is obtained.

For buckling analysis, the external in-plane uniaxial compression load is defined as follows:

$$N_x^e = -N_0 \quad (20)$$

Firstly by substituting of the Eq.(16) and Eq.(20) into Eq.(11) and then by applying non-dimensionalization procedure critical buckling load is obtained.

The kinematic components that provide the simply supported boundary condition in the free vibration analysis of the nanobeam examined in the xz-plane are as follows:

$$u(x) = A_m \cos\frac{m\pi x}{L}\sin\omega t$$

$$w(x) = C_m \sin\frac{m\pi x}{L}\sin\omega t$$

$$Lu_1(x) = D_m \cos\frac{m\pi x}{L}\sin\omega t \quad (21)$$

Firstly by substituting of the Eq.(21) into Eq.(11) and then by applying non-dimensionalization procedure an eigenvalue problem in matrix form is obtained as follows:

$$\left[K_{ij} - \Omega^2 M_{ij}\right]\begin{Bmatrix} A_m \\ C_m \\ D_m \end{Bmatrix} = \{0\} \quad (22)$$

where Ω is the frequency parameter corresponding to $\rho_c\omega^2$ and ρ_c represent mass density of ceramic component of the functionally graded material. The solution of the eigenvalue problem given by Eq.(22) gives the natural frequencies of the nanobeam.

3. Numerical results

The static bending, axial buckling, and free vibration analyses are carried out for functionally graded nanobeams whose material properties vary through the thickness direction according to a simple power rule. The solutions are obtained by the Navier method and hence for the simply supported boundary condition. The material properties considered in this study are given in Table 2.

Non-dimensionalization terms are used in the study as follows:

Uniformly distributed load;

$$\bar{w} = \frac{100E_cD_0}{q_0L^4}w \qquad \left(D_0 = \frac{E_ch^3}{12(1-\nu_c^2)}\right) \tag{23}$$

Table 2. Mechanical properties of component materials of functionally graded material which are considered in the study.

Component Material	Elasticity Modulus (GPa)	Poisson Ratio	Mass Density (kg/m^3)
SUS304 (Metal)	201.04	0.3262	8166
Si_3N_4 (Ceramic)	348.43	0.2400	2370

Point load applied to point x0 from x=0 to L:

$$\bar{w} = \frac{D_0}{q_0L^3}w \tag{24}$$

Critical buckling load:

$$\bar{N} = \frac{N_0L^2}{D_0} \tag{25}$$

Natural frequency parameter:

$$\Delta = \omega L^2\sqrt{\frac{\rho_c}{D_0}} \tag{26}$$

The thickness (h) of functionally graded nanobeam is 1 nm. Effects of the nonlocal parameter ($(e_0a)^2$), different material composition (p_z) and the beam geometry (length-to-thickness) on the bending, buckling, and vibration are investigated.

The comparison results for bending, buckling, and vibration are given in Table 3-7. The results obtained in this study are quite self-consistent among themselves. In addition, although a good agreement is observed in the comparison results, it is also seen that there are some differences between them. Although both of the generalized shear deformation theory and the Reddy theory are higher-order beam theories that take into account the effect of transverse shear deformation, which is neglected in classical beam theories. In this study, in-plane displacement components are also taken into account, leading to some differences between the results. However, the effect of Poisson's ratio on the mechanical behavior of beams is particularly significant in cases where the beam is subjected to out-of-plane deformation such as bending. In such cases, the beam experiences both tensile and compressive stresses along its length, as well as shear stresses across its cross-section. Poisson's ratio plays a crucial role in determining the deformation of the beam under these complex loading conditions. As it is seen in comparison results, considering the Poisson ratio in case of axial stress also affects the results. Because when the effect of Poisson's ratio is taken into account, the material exhibits a more rigid behavior. As a result, in the results obtained by considering the Poisson ratio, the bending deformation takes smaller values, while the critical buckling load and natural frequencies take larger values.

Table 3. Comparison of non-dimensional maximum center deflection of nanobeam under uniformly distributed load, (υ=0.3, $\bar{w} = \frac{100EI}{q_0L^4}w$, q_0=1).

$(e_0a)^2$	L/h=10			L/h=100		
	Ref. [5]	Present (without ν)	Present (with ν)	Ref. [5]	Present (without ν)	Present (with ν)
0	1.3346	1.3059	1.1913	1.3024	1.2735	1.1589
1	1.4622	1.4347	1.3088	1.4274	1.3992	1.2733
2	1.5898	1.5636	1.4264	1.5525	1.5249	1.3877
3	1.7174	1.6925	1.5440	1.6775	1.6506	1.5021
4	1.8450	1.8214	1.6616	1.8025	1.7763	1.6165

Table 4. Comparison of non-dimensional maximum center deflection of nanobeam under point load at center, (υ=0.3, $\bar{w} = \frac{100EI}{q_0L^3}w$, q_0=1).

$(e_0a)^2$	L/h=10			L/h=100		
	Ref. [4]	Present (without ν)	Present (with ν)	Ref. [4]	Present (without ν)	Present (with ν)
0	1.9878	2.0513	1.8713	1.9449	2.0005	1.8205
1	2.1564	2.2537	2.0560	2.1115	2.1979	2.0002
2	2.3250	2.4562	2.2406	2.2782	2.3954	2.1798
3	2.4936	2.6586	2.4253	2.4448	2.5928	2.3595
4	2.6623	2.8611	2.6100	2.6115	2.7903	2.5392

Table 5. Comparison of non-dimensional critical buckling load under uniaxial compression load, (υ=0.3, $\bar{N} = \frac{N_0L^2}{EI}$).

$(e_0a)^2$	L/h=10			L/h=100		
	Ref. [4]	Present (without ν)	Present (with ν)	Ref. [4]	Present (without ν)	Present (with ν)
0	9.6228	9.6226	10.5483	9.8671	9.8670	10.8425
1	8.7583	8.7582	9.6007	8.9807	8.9806	9.8686
2	8.0364	8.0363	8.8093	8.2405	8.2404	9.0551
3	7.4245	7.4244	8.1385	7.6130	7.6129	8.3656
4	6.8991	6.8990	7.5626	7.0743	7.0742	7.7736

Table 6. Comparison of non-dimensional fundamental frequencies, (υ=0.3, $\Delta = \omega L^2\sqrt{\frac{\rho}{EI}}$).

$(e_0a)^2$	L/h=10			L/h=100		
	Ref. [5]	Present (without ν)	Present (with ν)	Ref. [5]	Present (without ν)	Present (with ν)
0	9.7075	9.7071	10.1634	9.8679	9.8679	10.3442
1	9.2612	9.2608	9.6961	9.4143	9.4142	9.8687
2	8.8714	8.8709	9.2879	9.0180	9.0179	9.4532
3	8.5269	8.5265	8.9273	8.6678	8.6677	9.0861
4	8.2197	8.2193	8.6057	8.3555	8.3554	8.7588

Table 7. Comparison of first three non-dimensional fundamental frequencies, (L/h=5, υ=0.3, $\Delta = \omega L^2\sqrt{\frac{\rho}{EI}}$).

Modes	$(e_0a)^2$	Ref. [5]	Present (without ν)	Present (with ν)
1	0	9.2745	9.2690	9.6740
	1	8.8482	8.8429	9.2293
	2	8.4757	8.4706	8.8407
	3	8.1466	8.1417	8.4975
	4	7.8530	7.8484	8.1913
2	0	32.1847	31.9441	33.0538
	1	27.2519	27.0481	27.9878
	2	24.0589	23.8790	24.7086
	3	21.7765	21.6137	22.3646
	4	20.0407	19.8908	20.5818
3	0	61.5746	59.8105	61.3641
	1	44.8095	43.5257	44.6563
	2	36.9531	35.8943	36.8267
	3	32.1645	31.2430	32.0545
	4	28.8569	28.0301	28.7582

Table 8 and Table 9 show that the results of bending analysis of functionally graded nanobeam under uniformly distributed load and point load respectively. In all considered conditions in terms of material composition or geometry, maximum deflection increased with increasing nonlocal parameter value. This result confirms the nonlocal elasticity behavior of the considered material. The volume ratio exponent p_z determines the rate of change of the ceramic volume fraction from the lower surface to the upper surface; and as the p_z value increases, the ceramic volume ratio decreases, and the metal volume ratio increases. As a result, it can be said that the maximum deflection increases with increasing p_z value and therefore with increasing metal volume ratio. From the geometric point of view, the maximum deflection value decreases with the increase of L/h value; that is, the decrease in nanobeam thickness, in both loading conditions. However, in terms of all parameters examined, the beam with at least L/h=50 ratio is affected by all variation amounts.

According to the buckling results given in Table 10, the critical buckling load decreases as the p_z value and the nonlocal parameter value increase, so the material becomes softer. And, as the value of L/h increases, it increases; that is, the strength of the material against buckling increases.

The free vibration results for first three natural frequencies are presented in Table 11-Table 13. The natural frequencies decrease as the pz value and the nonlocal parameter value increase, but increase as the L/h value increases, similar to the buckling results. However, unlike the buckling results, vibration frequencies are less affected by the change of parameters. It can be thought that the reason for this is not an applied external force.

Table 8. Non-dimensional maximum center deflection under uniformly distributed load.

L/h	$(e_0a)^2$	Volume fraction exponent p_z						
		0	0.2	0.5	1	2	5	10
10	0	1.3063	1.4217	1.5418	1.6552	1.7496	1.8455	1.9260
	1	1.4352	1.5620	1.6940	1.8186	1.9223	2.0276	2.1160
	2	1.5641	1.7023	1.8461	1.9820	2.0949	2.2098	2.3061
	3	1.6930	1.8427	1.9983	2.1453	2.2676	2.3919	2.4962
	4	1.8220	1.9830	2.1505	2.3087	2.4403	2.5741	2.6863
20	0	1.2815	1.3949	1.5126	1.6227	1.7126	1.8031	1.8816
	1	1.4079	1.5326	1.6619	1.7829	1.8816	1.9810	2.0673
	2	1.5344	1.6703	1.8111	1.9431	2.0507	2.1590	2.2530
	3	1.6609	1.8080	1.9604	2.1032	2.2197	2.3370	2.4387
	4	1.7874	1.9457	2.1097	2.2634	2.3887	2.5149	2.6244
50	0	1.2745	1.3875	1.5044	1.6136	1.7023	1.7912	1.8691
	1	1.4003	1.5244	1.6529	1.7729	1.8703	1.9680	2.0536
	2	1.5261	1.6613	1.8013	1.9322	2.0383	2.1448	2.2381
	3	1.6519	1.7983	1.9498	2.0914	2.2063	2.3216	2.4226
	4	1.7777	1.9352	2.0983	2.2507	2.3743	2.4983	2.6070

Table 9. Non-dimensional maximum deflection under point load at center.

L/h	$(e_0a)^2$	Volume fraction exponent p_z						
		0	0.2	0.5	1	2	5	10
10	0	2.0519	2.2332	2.4219	2.6001	2.7482	2.8989	3.0253
	1	2.2544	2.4536	2.6609	2.8567	3.0195	3.1850	3.3239
	2	2.4569	2.6740	2.8999	3.1133	3.2907	3.4712	3.6225
	3	2.6594	2.8945	3.1390	3.3699	3.5620	3.7573	3.9211
	4	2.8620	3.1149	3.3780	3.6265	3.8332	4.0434	4.2197
20	0	2.0129	2.1912	2.3760	2.5490	2.6902	2.8323	2.9556
	1	2.2116	2.4075	2.6105	2.8006	2.9557	3.1118	3.2473
	2	2.4103	2.6237	2.8450	3.0522	3.2212	3.3914	3.5390
	3	2.6090	2.8400	3.0795	3.3038	3.4867	3.6709	3.8307
	4	2.8076	3.0563	3.3140	3.5553	3.7523	3.9505	4.1224
50	0	2.0020	2.1794	2.3631	2.5347	2.6739	2.8136	2.9360
	1	2.1996	2.3945	2.5963	2.7849	2.9378	3.0913	3.2258
	2	2.3972	2.6096	2.8296	3.0351	3.2018	3.3690	3.5156
	3	2.5948	2.8247	3.0628	3.2852	3.4657	3.6467	3.8054
	4	2.7924	3.0399	3.2960	3.5354	3.7296	3.9244	4.0952

Table 10. Non-dimensional critical buckling load under uniaxial compression load.

L/h	$(e_0a)^2$	Volume fraction exponent p_z						
		0	0.2	0.5	1	2	5	10
10	0	9.6197	8.8387	8.1502	7.5916	7.1823	6.8090	6.5245
	1	8.7556	8.0447	7.4180	6.9097	6.5371	6.1973	5.9384
	2	8.0339	7.3816	6.8066	6.3401	5.9983	5.6865	5.4489
	3	7.4221	6.8195	6.2883	5.8573	5.5415	5.2535	5.0340
	4	6.8969	6.3369	5.8433	5.4429	5.1494	4.8817	4.6778
20	0	9.8058	9.0081	8.3076	7.7436	7.3373	6.9692	6.6785
	1	8.9250	8.1989	7.5614	7.0480	6.6782	6.3431	6.0785
	2	98.1893	7.5231	6.9381	6.4671	6.1277	5.8203	5.5775
	3	7.5657	6.9502	6.4098	5.9746	5.6611	5.3771	5.1528
	4	7.0303	6.4584	5.9562	5.5518	5.2605	4.9966	4.7872
50	0	9.8593	9.0568	8.3528	7.7873	7.3819	7.0154	6.7229
	1	8.9736	8.2432	7.6025	7.0878	6.7188	6.3852	6.1190
	2	8.2339	7.5638	6.9758	6.5036	6.1650	5.8589	5.6146
	3	7.6069	6.9878	6.4446	6.0083	5.6955	5.4127	5.1871
	4	7.0686	6.4933	5.9886	5.5832	5.2925	5.0297	4.8200

Table 11. Non-dimensional fundamental natural frequency parameter.

L/h	$(e_0a)^2$	Volume fraction exponent p_z						
		0	0.2	0.5	1	2	5	10
10	0	9.7056	7.8369	6.6273	5.7806	5.1701	4.6857	4.4533
	1	9.2594	7.4766	6.3227	5.5149	4.9324	4.4703	4.2486
	2	8.8696	7.1618	6.0565	5.2827	4.7247	4.2821	4.0697
	3	8.5252	6.8837	5.8213	5.0776	4.5413	4.1158	3.9117
	4	8.2181	6.6357	5.6116	4.8947	4.3777	3.9675	3.7707
20	0	9.8277	7.9370	6.7131	5.8571	5.2414	4.7536	4.5178
	1	9.3759	7.5721	6.4045	5.5878	5.0004	4.5351	4.3101
	2	8.9811	7.2533	6.1348	5.3526	4.7899	4.3442	4.1286
	3	8.6324	6.9717	5.8966	5.1448	4.6039	4.1755	3.9683
	4	8.3214	6.7205	5.6842	4.9594	4.4380	4.0250	3.8253
50	0	9.8628	7.9658	6.7378	5.8791	5.2620	4.7732	4.5364
	1	9.4094	7.5996	6.4280	5.6089	5.0201	4.5538	4.3279
	2	9.0133	7.2797	6.1574	5.3727	4.8087	4.3621	4.1457
	3	8.6633	6.9970	5.9183	5.1641	4.6220	4.1927	3.9847
	4	8.3511	6.7449	5.7051	4.9781	4.4555	4.0416	3.8411

Table 12. Non-dimensional second natural frequency parameter.

L/h	$(e_0a)^2$	Volume fraction exponent p_z						
		0	0.2	0.5	1	2	5	10
10	0	37.0562	29.9004	25.2717	22.0217	19.6578	17.7734	16.8925
	1	31.3767	25.3177	21.3984	18.6465	16.6449	15.0493	14.3034
	2	27.7004	22.3513	18.8912	16.4618	14.6947	13.2861	12.6276
	3	25.0726	20.2309	17.0991	14.9001	13.3007	12.0257	11.4296
	4	23.0740	18.6183	15.7361	13.7124	12.2405	11.0671	10.5186
20	0	38.8226	31.3476	26.5095	23.1227	20.6804	18.7430	17.8133
	1	32.8724	26.5431	22.4464	19.5788	17.5108	15.8703	15.0831
	2	29.0208	23.4331	19.8165	17.2848	15.4591	14.0108	13.3159
	3	26.2677	21.2101	17.9366	15.6451	13.9926	12.6817	12.0526
	4	24.1739	19.5194	16.5068	14.3980	12.8772	11.6708	11.0919
50	0	39.3708	31.7973	26.8946	23.4662	21.0008	19.0481	18.1030
	1	33.3365	26.9238	22.7726	19.8696	17.7821	16.1286	15.3284
	2	29.4307	23.7692	20.1044	17.5416	15.6986	14.2389	13.5325
	3	26.6387	21.5143	18.1972	15.8775	14.2094	12.8881	12.2487
	4	24.5153	19.7994	16.7466	14.6119	13.0767	11.8608	11.2723

Table 13. Non-dimensional third natural frequency parameter.

L/h	$(e_0a)^2$	Volume fraction exponent p_z						
		0	0.2	0.5	1	2	5	10
10	0	77.8803	62.7809	53.0270	46.1532	41.0983	37.0424	35.2069
	1	56.6756	45.6874	38.5891	33.5869	29.9083	29.9567	25.6210
	2	46.7387	37.6770	31.8233	27.6981	24.6645	22.2304	21.1289
	3	40.6820	32.7946	27.6995	24.1088	21.4683	19.3497	18.3909
	4	36.4986	29.4222	24.8510	21.6297	19.2607	17.3599	16.4997
20	0	85.6191	69.1127	58.4315	50.9444	45.5245	41.2156	39.1720
	1	62.3073	50.2952	42.5222	37.0736	33.1294	29.9937	28.5065
	2	51.3830	41.4769	35.0668	30.5735	27.3208	24.7349	23.5085
	3	44.7245	36.1021	30.5226	26.6116	23.7804	21.5296	20.4621
	4	40.1253	32.3896	27.3839	23.8750	21.3350	19.3157	18.3579
50	0	88.2852	71.2985	60.3027	52.6114	47.0768	42.6913	40.5734
	1	64.2475	51.8858	43.8839	38.2868	34.2590	31.0676	29.5263
	2	52.9830	42.7887	36.1897	31.5739	28.2524	25.6205	24.3495
	3	46.1172	37.2439	31.5001	27.4824	24.5913	22.3005	21.1942
	4	41.3748	33.4140	28.2608	24.6563	22.0625	20.0073	19.0147

4. Conclusion

The aim of the study is to show that the nonlocal theory of elasticity is an effective tool for predicting the mechanical behavior of functionally graded nanobeams. The incorporation of nonlocal effects into models of bending, buckling, and vibration can provide valuable insights into the behavior of these structures and can aid in the design of advanced nanomaterials and devices. The material properties of functionally graded nanobeam were considered varying according to simple power law along the thickness direction. Effect of the nonlocal parameter ($(e_0a)^2$), variation of volume fraction exponent (p_z), and the geometrical parameters of nanobeam (length -to-thickness) on the bending under two types of loading conditions, buckling under uniaxial compression loading condition and free vibration were researched. The results show that this study is worthy of conduct, and especially in cases where the L/h value is below 50, the nonlocal parameter and the material volume fraction affect all the results more.

Authors Contribution: Conceive – B.U.; Design - B.U.; Supervision – B.U.; Experimental Performance, Data Collection and/or Processing – B.U.; Analysis and/or Interpretation – B.U.; Literature Review – B.U.; Writer - B.U.; Critical Reviews – B.U.

Conflicts Of Interest: The authors have decl ared no conflicts of interest.

Orcid-ID

Bahar UYMAZ https://orcid.org/0000-0002-0036-0730

Reference

[1] Talizina N.F. Managing the process of learning. Moscow State University Publishing House. – 1975, 342 c.

[2] Leontyev L.P., Gohman O.G. Problems of management of educational processes: Mathematical models. - Riga, 1984. – 239 c.

[3] R. S. Sutton and A. G. Barto, Reinforcement Learning: An Introduction, MIT Press, Cambridge, MA, USA, 1998.

[4] Mayer R.B. Cybernetic pedagogy: Simulation of the learning process. - Eyes: GGPI, 2013. – 138 c.

[5] Pontryagin, L.S.; Boltyanskii, V.G.; Gamkrelidze, R.V.; Mishchenko, E.F. Pontryagin Selected Works: The Mathematical Theory of Optimal Process; Gordon and Breach Science Publishers: NY, USA, 1985; Volume 4, p. 360.

[6] Pivneva S. V. Modeling of discrete optimization problems / S. V. Pivneva, M. A. Trifonov // Vector of Science. - No. 3 (13), 2010. - pp. 31-34. (in Russian)

[7] Porter B., Grossley R. Modal Control. Theory and Applications. London: Taylor and Francis, 1972.

[8] Volgin L.N. Optimal discrete control of dynamical systems. M. Science, 1986, 240p (in Russian)

[9] Dumachev VN Fundamentals of control theory. 2015, 383p (in Russian)

[10] Vasiliev E.M., Gusev K.Yu. Modal control of non-stationary systems // Bulletin of the Voronezh State Technical University. 2008. V. 4. No. 8. pp. 46-54. (in Russian)

[11] Makkapati, V.R.; Dor, M.; Tsiotras, P. Trajectory desensitization in optimal control problems. In Proceedings of

the IEEE Conference on Decision and Control, Miami, FL, USA, 17–19 December 2018; pp. 2478–2483.